

# Mechanisms responsible for the inhibitory effects of epothilone B on scar formation after spinal cord injury

Wei Zhao<sup>1</sup>, Yong Chai<sup>2</sup>, Yun Hou<sup>3</sup>, Da-wei Wang<sup>1</sup>, Jian-qiang Xing<sup>1</sup>, Cheng Yang<sup>2\*</sup>, Qing-min Fang<sup>1,\*</sup>

1 Department of Spinal Surgery, Binzhou Medical University Hospital, Binzhou, Shandong Province, China

2 Department of Anatomy, Binzhou Medical University, Yantai, Shandong Province, China

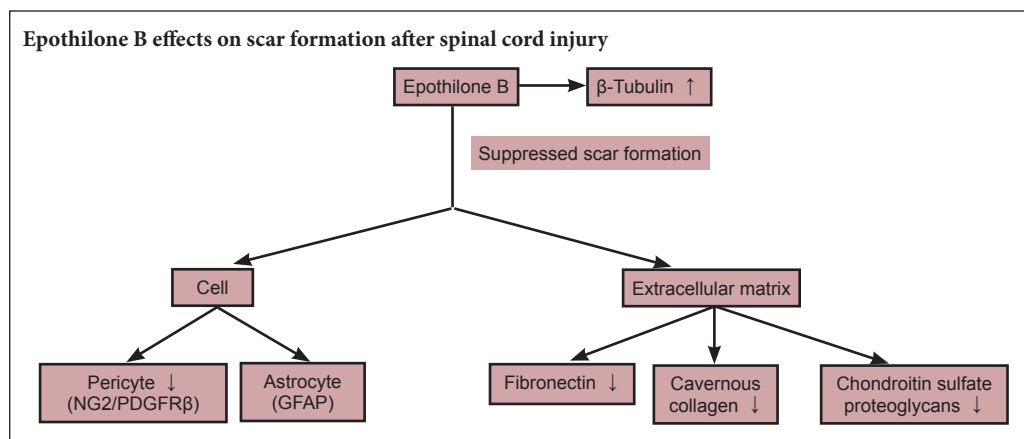
3 Department of Histology and Embryology, Binzhou Medical University, Yantai, Shandong Province, China

**How to cite this article:** Zhao W, Chai Y, Hou Y, Wang DW, Xing JQ, Yang C, Fang QM (2017) Mechanisms responsible for the inhibitory effects of epothilone B on scar formation after spinal cord injury. *Neural Regen Res* 12(3):478-485.

**Open access statement:** This is an open access article distributed under the terms of the Creative Commons Attribution-NonCommercial-ShareAlike 3.0 License, which allows others to remix, tweak, and build upon the work non-commercially, as long as the author is credited and the new creations are licensed under the identical terms.

**Funding:** This work was supported by a grant from the Science and Technology Developing Program of Shandong Provincial Government of China, No. 2010GSF10254; a grant from the Medical and Health Science and Technology Plan Project of Shandong Province of China, No. 2015WS0504.

## Graphical Abstract



\*Correspondence to:  
Cheng Yang, M.D. or  
Qing-min Fang,  
yangchxn@163.com or  
byfqm2008@163.com.

orcid:  
0000-0002-7898-8376  
(Cheng Yang)  
0000-0002-8388-8740  
(Qing-min Fang)

doi: 10.4103/1673-5374.202921

Accepted: 2017-02-06

## Abstract

Scar formation after spinal cord injury is regarded as an obstacle to axonal regeneration and functional recovery. Epothilone B provides moderate microtubule stabilization and is mainly used for anti-tumor therapy. It also reduces scar tissue formation and promotes axonal regeneration after spinal cord injury. The aim of the present study was to investigate the effect and mechanism of the microtubule-stabilizing reagent epothilone B in decreasing fibrotic scarring through its action on pericytes after spinal cord injury. A rat model of spinal cord injury was established via dorsal complete transection at the T<sub>10</sub> vertebra. The rats received an intraperitoneal injection of epothilone B (0.75 mg/kg) at 1 and 15 days post-injury in the epothilone B group or normal saline in the vehicle group. Neuron-gial antigen 2, platelet-derived growth factor receptor  $\beta$ , and fibronectin protein expression were dramatically lower in the epothilone B group than in the vehicle group, but  $\beta$ -tubulin protein expression was greater. Glial fibrillary acidic protein at the injury site was not affected by epothilone B treatment. The Basso, Beattie, and Bresnahan locomotor scores were significantly higher in the epothilone B group than in the vehicle group. The results of this study demonstrated that epothilone B reduced the number of pericytes, inhibited extracellular matrix formation, and suppressed scar formation after spinal cord injury.

**Key Words:** nerve regeneration; spinal cord injury; epothilone B; pericytes; gene expression; fibrous scar;  $\beta$ -tubulin; platelet-derived growth factor receptor  $\beta$ ; neuron-gial antigen 2; fibronectin; glial fibrillary acidic protein; rats; neural regeneration

## Introduction

Spinal cord injury (SCI) causes neurodegeneration and failure of axonal reinnervation to the target organ (Pannek et al., 2016). Little progress has been made in the treatment of SCI because of the limited understanding of the pathophysiological mechanisms. The pathological process of SCI

involves four different reaction stages: neural cell death, hypertrophic scarring, axonal degeneration, and destruction of the microvasculature. Neurons in the adult central nervous system are thought to have limited repair or regeneration capability (Bjorklund and Lindvall, 2000). Poor intrinsic axonal growth capacity and fibrotic scar formation are major

obstacles to the recovery of spinal cord function (Salgado et al., 2015). An ideal treatment of SCI would involve reduction of fibrotic scarring (Klapka et al., 2005; Xue et al., 2015), secretion of more factors that promote axonal growth (Schnell and Schwab, 1990; Bradbury et al., 2002; GrandPre et al., 2002), and enhancement of the axonal regeneration capacity (Liu et al., 2010; Alilain et al., 2011; Lu et al., 2012).

Most studies of the scar tissue that forms at injury sites have focused on astrocytes, and such scars are often referred to fibrotic scars (Silver and Miller, 2004; Fawcett, 2006; Okada et al., 2006; Rolls et al., 2009; Sofroniew, 2009; Fan et al., 2016). However, a specific subtype of stromal cell, the pericyte, plays a major role in scar formation (Goritz et al., 2011; Tempel et al., 2013). Newly developed pharmaceuticals that specifically target pericytes in SCI are expected to affect neuronal regeneration and long-term recovery of neurological function.

Two microtubule-stabilizing reagents, paclitaxel and epothilone B (EpoB), were recently reported to reduce scarring and promote axonal growth in rodent SCI models (Hellal et al., 2011; Sengottuvel et al., 2011; Crunkhorn et al., 2015; Ruschel et al., 2015). However, the cellular mechanisms mediating these effects remain unclear. In *in vitro* wound-healing assays, EpoB elevated the levels of stable detyrosinated microtubules by diminishing fibroblast polarization and migration to the injury site and promoting axonal regeneration (Ruschel et al., 2015). Paclitaxel does not traverse the blood-brain barrier (Fellner et al., 2002) and therefore cannot be used in the clinical setting. EpoB is a microtubule-stabilizing drug to which the blood-brain barrier is permeable (Ballatore et al., 2012). EpoB-treated rats were compared with vehicle-treated rats, and no adverse effects were observed (Ruschel et al., 2015). However, the effects of EpoB on pericytes in scarring after SCI, as well as the associated mechanisms underlying the improvements in SCI-related symptoms, remain incompletely understood.

In the present study, we investigated the effect of EpoB on decreased scar formation and observed its effect on pericytes in the treatment of SCI in rats. We also investigated the possible mechanisms of scarring following EpoB administration in a model of SCI and further confirmed the effects of EpoB on mitigation of scar formation and improvement in locomotor capability after SCI.

## Materials and Methods

### Animals

All animal experiments were performed in compliance with the Chinese Association for Laboratory Animal Sciences. Thirty-eight adult female Sprague-Dawley rats weighing 220–250 g and aged 10–12 weeks were purchased from the Experimental Animal Center at Shandong Green Leaf Pharmaceutical Co., Ltd., China (SYXK (Lu) 20140003, Yantai, China). All experiments involving rats were approved by the Ethics Committee for Animal Care and Use of Binzhou Medical University in China (2014-09-20). Every effort was made to minimize the number and suffering of the animals used in the following experiments in accordance with the

United States National Institutes of Health Guide for the Care and Use of Laboratory Animals (NIH Publication No. 85-23, revised 1986).

### SCI model establishment and drug administration

The surgical procedures were performed in accordance with the guiding principles for experimental animal wellness of the Ministry of Science and Technology of the People's Republic of China (2006) and ARRIVE guideline (Kilkenny et al., 2010).

The rats ( $n = 38$ ) were randomly divided into three groups: the control ( $n = 6$ ), vehicle ( $n = 16$ ), and EpoB ( $n = 16$ ) groups. The rats in the vehicle and EpoB groups were deeply anesthetized by an intraperitoneal injection of 4% chloral hydrate and underwent dorsal complete transection at the T<sub>10</sub> vertebra. They then received an intraperitoneal injection of EpoB at 0.75 mg/kg (Dalian Meilun Biology Technology Co., Ltd., China) or vehicle (1:1 mixture of dimethyl sulfoxide and saline) at 1 and 15 days post-injury (Ruschel et al., 2015). The rats in the control group were only deeply anesthetized and intraperitoneally injected with normal saline; no surgical procedures were performed. An SCI model was thus surgically established (Zhang et al., 2015). The post-operative care was conducted according to a previous study (Chen et al., 2000).

### Behavioral analysis

Functional assessment was performed using the Basso, Beattie, and Bresnahan (BBB) locomotor recovery scale (Basso et al., 1995) at 3, 7, 14, and 21 days postoperatively. The locomotor function of the rats' posterior limbs after surgical establishment of SCI was evaluated by two trained examiners in a double-blind manner. In brief, the rats were tested by two independent examiners 24 hours after the surgery and then weekly for 3 consecutive weeks. The two examiners' scores for each rat were averaged; the scores ranged from 0 (no movement) to 21 (normal movement). Each session lasted for 4 minutes (Zhang et al., 2015).

### Tissue collection and processing

The rats used for the morphological study were deeply anesthetized by an intraperitoneal injection of 4% chloral hydrate and perfused with 0.9% saline solution (37°C; 300 mL) through the heart followed by 4% paraformaldehyde in 0.01 M phosphate buffer (pH 7.4) at 4°C (300 mL). The spinal cord of the thoracic spinal segment T<sub>10</sub> vertebra was dissected and post-fixed in 4% paraformaldehyde at 4°C for 6 hours. For paraffin sectioning, the tissues were dehydrated through a graded alcohol series, permeabilized with xylene, embedded in paraffin, and sectioned.

### Masson's trichrome staining

For Masson's trichrome staining, the tissue sections were deparaffinized with water, treated with a Masson staining fluid (Fuzhou Maixin Biotech Co., Ltd., Fuzhou, China) for 5 minutes, washed with distilled water, incubated with aniline blue, differentiated in a differentiation liquid, rewashed

in distilled water, dehydrated through a graded alcohol series, permeabilized with xylene, and mounted with neutral balsam.

### Immunofluorescence staining

The following primary antibodies were used: mouse anti-neuron-glia antigen 2 (anti-NG2) (1:200, ab50009; Abcam, Cambridge, UK), rabbit anti-platelet-derived growth factor receptor  $\beta$  (anti-PDGFR $\beta$ ) (1:100, ab32570; Abcam), rabbit polyclonal anti-glia fibrillary acidic protein (anti-GFAP, 1:100, ZA-0117; Beijing Zhongshan Golden Bridge Biotechnology Co., Ltd., Beijing, China), rabbit anti- $\beta$ -tubulin (9F3) (1:200, #2128; Cell Signaling Technology, Inc., Danvers, MA, USA), and rabbit polyclonal anti-fibronectin (1:100, ab2413; Abcam). The secondary antibodies were Dylight 549-conjugated goat anti-rabbit IgG (1:400, #A23320; Abbkine, CA, USA) and fluorescein isothiocyanate-conjugated goat anti-mouse IgG (FITC, 1:400, #A22110; Abbkine, CA, USA). The immunofluorescent staining was performed as previously described (Zhang et al., 2015). In brief, paraffin-embedded sections were deparaffinized, rehydrated, and washed three times with 0.01 M phosphate-buffered saline (PBS). The tissue section slides were treated with citric acid buffer (0.01 M, pH 6.0), microwaved at full power for 10 minutes for antigen retrieval, and naturally cooled to room temperature. After washing three times with 0.01 M PBS, the slides were incubated with 0.01 M PBS containing 0.05% Triton X-100 for 15 minutes at room temperature, washed three times with 0.01 M PBS, and incubated with 5% normal goat serum to block nonspecific staining for 30 minutes at 37°C. Incubation with the appropriate primary antibodies was performed overnight at 4°C. Following repeated washing with 0.01 M PBS, the sections were incubated with respective secondary antibodies for 30 minutes at 37°C in the dark. The nuclei were counterstained using DAPI (1:1,000) and repeatedly washed with 0.01 M PBS. Pericytes were examined by double immunofluorescence staining of NG2 and PDGFR $\beta$ . The primary antibodies (mouse anti-NG2 and rabbit anti-PDGFR $\beta$ ) were performed together, like the secondary antibodies. After washing, the slides were mounted with a coverslip and examined under a confocal microscope (TCS SPE; Leica, Wetzlar, Germany). The scar formation of NG2, PDGFR $\beta$ , GFAP,  $\beta$ -tubulin, and fibronectin immunoreactivity in the anterior horn of the spinal cord was analyzed using Image-Pro Plus software (Media Cybernetics, Rockville, MD, USA).

### Western blot assay

The fresh spinal cord tissues of spinal cord segment T<sub>10</sub> were homogenized in RIPA lysis buffer (Solarbio, Beijing, China) according to the manufacturer's instructions. The lysates were centrifuged at 12,000 r/min for 10 minutes at 4°C, and the protein concentration of the supernatants was determined with a bicinchoninic acid protein assay kit (Solarbio). Fifty micrograms of protein from each sample was mixed with 2 $\times$  sodium dodecyl sulfate polyacrylamide gel electrophoresis loading buffer and denaturalized by heating at 95°C for 5 minutes. The proteins were electrophoresed on 10%

sodium dodecyl sulfate polyacrylamide gels and transferred onto a polyvinylidene difluoride membrane. After blocking in Tris-buffered saline and Tween 20 (TBST) containing 5% skimmed milk for 4 hours, the membranes were incubated overnight at 4°C with the following primary antibodies in TBST containing 5% skimmed milk (anti-NG2, 1:2,000, ab50009, Abcam; anti-PDGFR $\beta$  1:5,000, ab32570, Abcam; anti- $\beta$ -tubulin, 1:1,000, #2128, Cell Signaling Technology, Inc.; anti-fibronectin, 1:1,000, ab2413, Abcam; anti-GFAP, 1:1,000, #3670, Cell Signaling Technology, Inc.; anti- $\beta$ -actin, 1:5,000, Sigma). After washing, the blot membranes were incubated with horseradish peroxidase-conjugated secondary antibody (1:2,000, goat anti-rabbit IgG and goat anti-mouse IgG; Sigma, Carlsbad, CA, USA) in TBST for 1 hour and developed in an enhanced chemiluminescence detection reagent mixture (Novland BioPharma, Shanghai, China). The absorbance of the scanned bands was determined using Image J software (National Institutes of Health, Rockville, MD, USA). Protein levels were represented as the ratio of the relative grayscale value for the protein of interest to that of  $\beta$ -actin.

### Real-time quantitative reverse transcription polymerase chain reaction (qRT-PCR)

Total RNA was extracted from the spinal cord samples with TRIzol according to manufacturer's instruction. According to the manual of the TaqMan MicroRNA Reverse Transcriptase Kit, qRT-PCR was performed using the PrimeScript™ RT Master Mix with MX3000P real-time PCR system. The relative expression of the target genes was calculated by the  $2^{-\Delta\Delta Ct}$  method (Livak and Schmittgen, 2001). The primers for qRT-PCR are listed in **Table 1**.

### Statistical analysis

Data, expressed as the mean  $\pm$  SD, were analyzed using GraphPad Prism 5 software (GraphPad Software, Inc., La

**Table 1 Primers used for real-time quantitative reverse transcription polymerase chain reaction**

Name	Sequence (5'-3')	Product size (bp)
NG2	Forward: CCC TGG CTC CACT ACA ACT G	102
	Reverse: CTG CCT CCT GGA CTA CCT C	
PDGFR $\beta$	Forward: GTC AAT GTC CCT GTC CGT GT	157
	Reverse: GTG TGG GTG ACA GTT TTC GC	
GFAP	Forward: AGA AAA CCG CAT CAC CAT TCC	125
	Reverse: TCT CCA CCG TCT TTA CCA CG	
Fibronectin	Forward: AAG AGG CAG GCT CAG CAA AT	116
	Reverse: GTC CGT TCC CAC TGC TGA TT	
$\beta$ -tubulin III	Forward: GAC GCC AAG AAC ATG ATG GC	183
	Reverse: GTC ACA CAC CGC TAC CTT GA	
$\beta$ -Actin	Forward: CGT AAA GAC CTC TAT GCC AAC A	131
	Reverse: GGA GGA GCA ATG ATC TTG ATC T	

NG2: Neuron-glia antigen 2; PDGFR $\beta$ : platelet-derived growth factor receptor  $\beta$ ; GFAP: glia fibrillary acidic protein.

Jolla, CA, USA). Multiple group comparisons of differences in quantitative measurements were made using one-way analysis of variance, and Dunnett's test was used to compare differences among groups. All assays were repeated at least three times for each sample. A value of  $P < 0.05$  was considered statistically significant.

## Results

### Effects of EpoB on scar formation

Histological examinations were performed to examine the effect of EpoB treatment on scar formation after contusion at the SCI site. Masson's trichrome staining was performed on the spinal cord in both cross sections and longitudinal sections. Hemorrhage, edema, necrosis, axonal degeneration, demyelination, inflammatory cell infiltration, and glial cell response were seen in the area surrounding the SCI site in both the vehicle and EpoB groups at 3 and 21 days post-SCI. The cavernous collagen content was significantly higher in the vehicle group than in the EpoB group, and hypertrophic scarring was significantly reduced in the EpoB group (Figure 1A–D). Fibronectin staining revealed less expression in the EpoB than vehicle group; this was further verified with protein expression level quantification. The levels of fibronectin were lower in the spinal cord of the control group and significantly increased at 3 days ( $P < 0.01$ ) and 21 days ( $P < 0.001$ ) after SCI. Compared with the vehicle group, the fibronectin levels were significantly lower in the EpoB group at both 3 days ( $P < 0.01$ ) and 21 days ( $P < 0.05$ ) (Figure 1E–H, Q–R). No significant differences in GFAP staining or expression were observed between the vehicle and EpoB groups. Compared with the control group, the GFAP levels were significantly higher in the vehicle group at 3 days ( $P < 0.01$ ) and 21 days ( $P < 0.05$ ); there was no significant difference between the vehicle and EpoB groups (Figure 1I–L, Q–R). The  $\beta$ -tubulin staining was stronger in the EpoB group than in the vehicle group. The quantified expression was significantly higher in the EpoB than in the vehicle group at 3 days ( $P < 0.05$ ) and 21 days ( $P < 0.05$ ) (Figure 1M–P, Q–R).

### Effects of EpoB on NG2 and PDGFR $\beta$ expression in the injured spinal cord

Although full evaluation of pericytes requires a combination of criteria regarding location, morphology, and gene/protein expression patterns, we utilized the most widely accepted expression markers, NG2 and PDGFR $\beta$  (Armulik et al., 2011), to assess the correlation between the scarring process and pericytes. The number of NG2-immunoreactive cells was higher in the vehicle group than in the EpoB group (Figure 2A–D). The protein expression levels of NG2 were significantly higher in the vehicle group than in the control group at 3 days ( $P < 0.01$ ) and 21 days ( $P < 0.01$ ) but were significantly lower in the EpoB group than in the vehicle group at both 3 days ( $P < 0.01$ ) and 21 days post-SCI ( $P < 0.05$ ) (Figure 2I–J). The number of PDGFR $\beta$ -immunoreactive cells was decreased in the EpoB group at both 3 and 21 days post-SCI (Figure 2E–H). The protein expression level was also decreased as shown by western blot assay (Figure 2I–J). The

expression levels of PDGFR $\beta$  were lower in the EpoB group than in the vehicle group at 21 days ( $P < 0.05$ ) and significantly higher in the vehicle group than in the control group ( $P < 0.01$ ). EpoB suppressed expression of the pericyte markers NG2 and PDGFR $\beta$  during scar formation.

### Effects of EpoB on expression levels of GFAP, fibronectin, $\beta$ -tubulin III, NG2, PDGFR $\beta$ mRNA in the injured spinal cord

To further explore the effects of EpoB on scar formation through gene expression regulation or protein degradation, qRT-PCR for GFAP, fibronectin,  $\beta$ -tubulin III, NG2, and PDGFR $\beta$  was carried out at four time points post-SCI. Here, only the 3- and 21-day post-SCI measurements are shown. GFAP mRNA expression was higher in the vehicle group than in the control group at 3 days ( $P < 0.01$ ) and 21 days ( $P < 0.01$ ), but there was no significant difference between the vehicle and EpoB groups. Fibronectin expression was significantly higher in the vehicle group than in the control group at 3 days ( $P < 0.01$ ) and 21 days ( $P < 0.01$ ) but was significantly lower in the EpoB than vehicle group at 3 days ( $P < 0.05$ ) and 21 days ( $P < 0.05$ ). The expression of  $\beta$ -tubulin III was significantly higher in the EpoB group than in the control and vehicle groups at 3 days ( $P < 0.01$ ) and 21 days ( $P < 0.01$ ) (Figure 3A). NG2 mRNA expression was significantly higher in the vehicle group than in the control group at 3 days ( $P < 0.01$ ) and 21 days ( $P < 0.001$ ) and higher than in the EpoB group at 3 days ( $P < 0.05$ ) and 21 days ( $P < 0.01$ ) post-SCI. PDGFR $\beta$  mRNA expression was also significantly higher in the vehicle group than in the control group at 3 days ( $P < 0.001$ ) and 21 days ( $P < 0.01$ ) and higher than in the EpoB group at 3 days ( $P < 0.001$ ) and 21 days ( $P < 0.01$ ) post-SCI (Figure 3B). These findings indicate that EpoB regulates gene expression during scar formation.

### Effects of EpoB on motor function after SCI

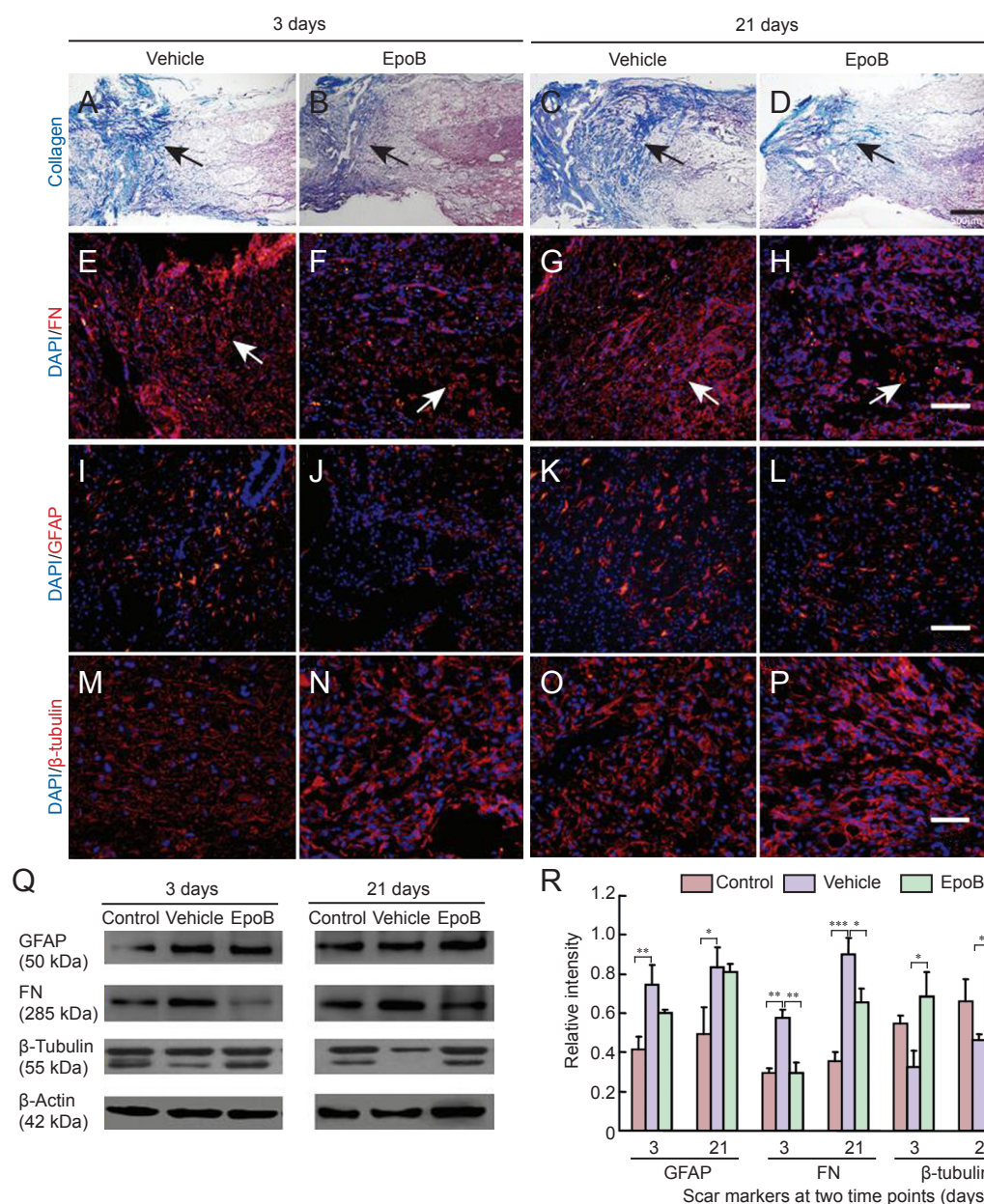
The rats with SCI exhibited paralysis and urinary incontinence, while the control rats displayed normal behavior. To reveal the effect of EpoB treatment on the improvement of post-SCI symptoms, the rats were assessed with the BBB locomotor rating scale at four time points from 1 to 3 weeks after surgery as described previously (Zhang et al., 2015). The BBB scores gradually increased over time in both the vehicle and EpoB groups throughout the entire follow-up period, while the BBB scores were significantly higher in the EpoB group than in the vehicle group at 2 to 3 weeks post-SCI (Figure 3C).

### Effects of EpoB on pericyte number at injury site

Pericytes were examined by double immunofluorescence staining of NG2 and PDGFR $\beta$ . The number of pericytes was slightly increased at 3 days post-injury. The number of pericytes was significantly increased in the vehicle group but significantly decreased in the EpoB group at 21 days post-injury (Figure 4).

## Discussion

The scar-induced barrier to axonal reconnection must be



(A–D) Masson’s trichrome staining of the SCI site at different time points. At both time points, the collagenous staining (blue, arrows) was weaker in the EpoB group (SCI + EpoB) than in the (normal saline) vehicle group at (A, B) 3 days post-SCI and (C, D) 21 days post-SCI. Blue staining indicates collagenous material, and red or dark red staining indicates nervous tissue. (E–H) The FN immunofluorescent staining (red, arrows) was reduced in the EpoB group at both (E, F) 3 days post-SCI and (G, H) 21 days post-SCI. (I–L) GFAP staining (red) did not show an apparent difference. (M–P) The β-tubulin staining (red) was stronger in the EpoB group than in the vehicle group. Nuclei are stained with DAPI (blue). Scale bars: (A–D) 500 μm, (E–H) 100 μm, (I–L) 100 μm, and (M–P) 50 μm. (Q, R) Western blot analysis and quantification (gray value: marker/β-actin) confirmed the histochemical staining results. \**P* < 0.05, \*\**P* < 0.01, \*\*\**P* < 0.001. Data are expressed as the mean ± SD (*n* = 3; one-way analysis of variance followed by Dunnett’s test). EpoB: Epopithilone B; SCI: spinal cord injury; GFAP: glial fibrillary acidic protein; DAPI: 4’,6-diamidino-2-phenylindole; FN: fibronectin.

**Figure 1** Effects of EpoB on responsive scar formation at the injury site.

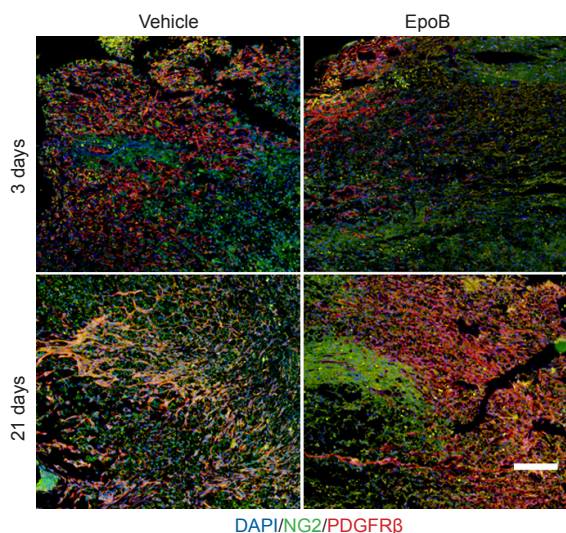
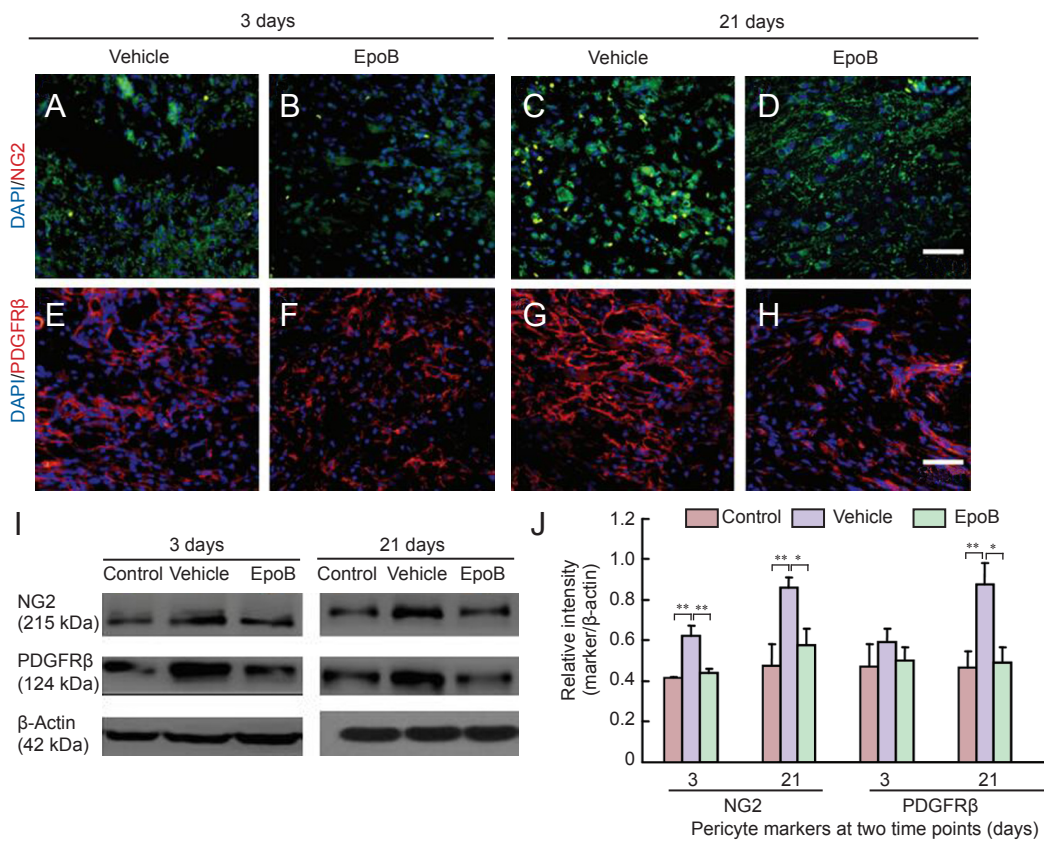


**Figure 4** Effects of EpoB on number of pericytes in the injured spinal cord. Immunofluorescence staining of the injury site at 3 and 21 days and examination under a confocal microscope. Pericytes were examined by double immunofluorescence staining for NG2 (green) and PDGFRβ (red). At 3 days post-injury, the number of pericytes showed a small increase; they were significantly increased at 21 days post-injury in the vehicle group (normal saline). However, after EpoB treatment, the number of pericytes was decreased. Nuclei are stained with DAPI (blue). Scale bar: 200 μm. EpoB: Epopithilone B; NG2: neuron-glia antigen 2; PDGFRβ: platelet-derived growth factor receptor β; DAPI: 4’,6-diamidino-2-phenylindole.



(A–H) Immunofluorescence staining of the SCI site at different time points and examination under a confocal microscope. (A–D) Number of NG2 (green)-immunoreactive cells was higher in the vehicle group than in the EpoB group. (E–H) Number of PDGFRβ (red)-immunoreactive cells was higher in the vehicle group (normal saline) than in the EpoB group (SCI + EpoB). Nuclei are stained with DAPI (blue). Scale bars: (A–H) 50 μm. (I, J) The quantification (gray value ratio of marker/β-actin) confirmed the histochemical staining results: the NG2 and PDGFRβ expression levels were decreased in the EpoB group. \* $P < 0.05$ , \*\* $P < 0.01$ . Data are expressed as the mean ± SD ( $n = 3$ ; one-way analysis of variance followed by Dunnett's test). FN: Fibronectin; NG2: neuron-glia antigen 2; PDGFRβ: platelet-derived growth factor receptor β; EpoB: epothonone B; DAPI: 4',6-diamidino-2-phenylindole.

**Figure 2** Expression of NG2, PDGFRβ in injured spinal cord after treatment with EpoB.

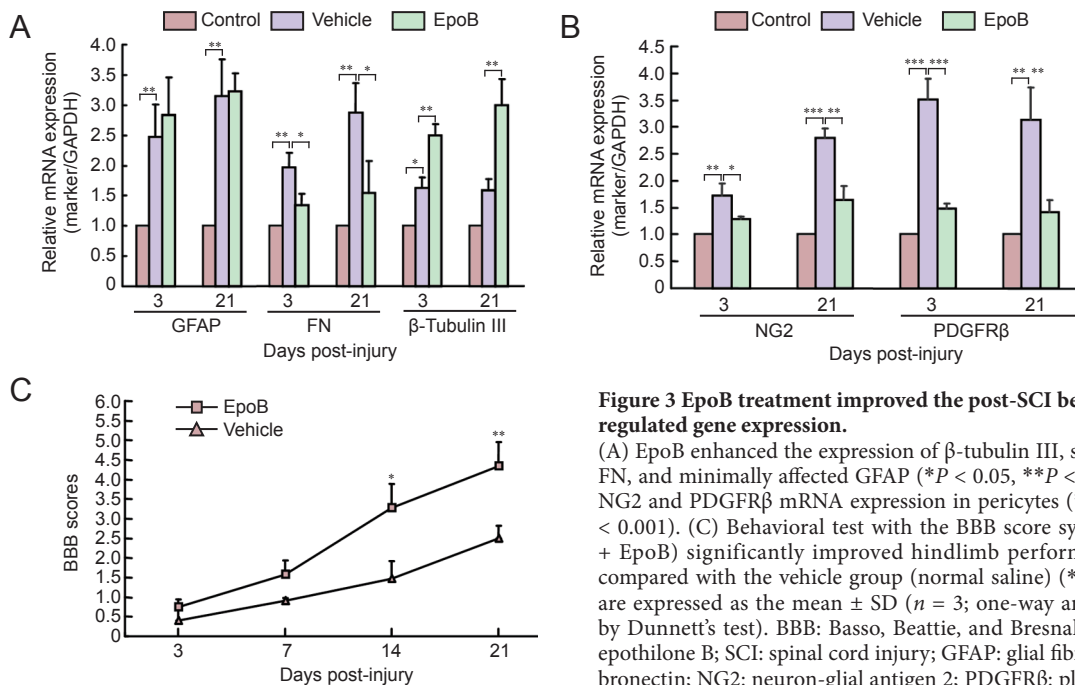


**Figure 3** EpoB treatment improved the post-SCI behavior recovery and regulated gene expression.

(A) EpoB enhanced the expression of β-tubulin III, suppressed the expression of FN, and minimally affected GFAP (\* $P < 0.05$ , \*\* $P < 0.01$ ). (B) EpoB suppressed NG2 and PDGFRβ mRNA expression in pericytes (\* $P < 0.05$ , \*\* $P < 0.01$ , \*\*\* $P < 0.001$ ). (C) Behavioral test with the BBB score system. EpoB treatment (SCI + EpoB) significantly improved hindlimb performance at 2 weeks post-SCI compared with the vehicle group (normal saline) (\* $P < 0.05$ , \*\* $P < 0.01$ ). Data are expressed as the mean ± SD ( $n = 3$ ; one-way analysis of variance followed by Dunnett's test). BBB: Basso, Beattie, and Bresnahan locomotor scale; EpoB: epothonone B; SCI: spinal cord injury; GFAP: glial fibrillary acidic protein; FN: fibronectin; NG2: neuron-glia antigen 2; PDGFRβ: platelet-derived growth factor receptor β.

overcome to establish effective therapy for SCI. Such scars are mainly composed of astrocytes and proteoglycans. Astrocytes are the reactive, responsive cells (Silver and Miller, 2004; Sofroniew, 2009; Li et al., 2016). Myofibroblasts are currently considered to be the dominant collagen-producing cells in the scarring process. Myofibroblasts originate

from local resident fibroblasts, bone marrow cells, endothelial-to-mesenchymal transition cells, and pericytes (Lebleu et al., 2013). Scar formation in SCI is a type of whole-body fibrosis. Mesenchymal cells, including microvascular mural cells (pericytes), are major progenitors of scar-forming myofibroblasts in the kidney and other organs, in which

lipoprotein receptor-related proteins 6 is a co-receptor for multiple fibrogenic signaling pathways in pericytes and myofibroblasts (Ren et al., 2013). However, using a cell fate tracing strategy, Lebleu et al. (2013) determined that vascular pericytes probably do not contribute to the emergence of myofibroblasts or fibrosis in the kidney. This finding contrasts other observations that type 1 pericytes are the major scar-forming cells in SCI; blocking the generation of progeny of this pericyte subtype results in failure to seal the injured tissue (Goritz et al., 2011). The formation of connective tissue is common to many injuries and pathologies. The development of fibrosis in different organs and at different sites (e.g., bone marrow, kidney, lung, and SCI) makes it difficult to assume that the fibrosis originates from the same type of cells. Instead, different types of pericytes might have different functions at different stages, or transformation from pericytes to myofibroblasts might occur. Whether myofibroblasts and pericytes simply act at different phases during scar formation or are simultaneously involved in the final stage of fibrosis remains unknown. A single-cell gene profiling study will help to clarify this issue. In the present study, both fibroblasts and pericytes were actively involved in recovery of the spinal cord after SCI.

It is difficult to meet every criterion for the current definition of pericytes, and practical application is not easy. The following molecular markers have been suggested: PDGFR $\beta$  (CD140b), NG2,  $\alpha$  smooth muscle actin, desmin, vimentin, RGS-5, 3G5, Kir6.1, nestin, Sca-1, aminopeptidases A and N, high-molecular-weight melanoma-associated antigen, alkaline phosphatase,  $\gamma$ -glutamyl transpeptidase, butyrylcholinesterase, FcR, CD4, CD11b, CD34, CD140a, and MHC classes I and II (Armulik et al., 2011; Kamouchi et al., 2011). We chose the most commonly used parameters, PDGFR $\beta$  and NG2, to represent pericytes, and we used fibronectin and collagen as fibroblast markers (Stallcup, 2002; Bergers and Song, 2005; Kucharova et al., 2011; Winkler et al., 2012). Our results revealed that EpoB stabilized microtubulin by elevating the levels of dephosphorylated and acetylated tubulin as demonstrated by Bradke's group (Ruschel et al., 2015), and the total microtubulin content was significantly elevated after EpoB treatment. Two steps are necessary to establish an effective therapeutic strategy for recovery of neurological function after SCI: first, to determine which cell type is involved in scar formation at different post-SCI stages, and second, to further define the molecules that are involved in the biochemical pathway controlling scar formation and neuronal axon regeneration and that establish the right connection to the target organ. A single-cell profiling study is necessary. Scar tissue is mainly composed of three types of cells: astrocytes/oligodendrocytes, fibroblasts, and stromal cells. Astrocytes participate in a reactive response to the injury by secreting chondroitin and keratin sulfate proteoglycans (Silver and Miller, 2004). The astrocyte has long been believed to be a key cell type involved in scar formation, but the present study showed no significant difference in the astrocyte marker GFAP between the vehicle and EpoB groups; this

suggests that astrocytes do not play a supporting role in scar formation but instead act as inflammatory cells. The fibronectin and laminin contents are rich in the fibrotic scar tissue that forms after SCI (Hellal et al., 2011); chondroitin sulfate proteoglycans are inhibitory factors (de Castro et al., 2005; Klapka et al., 2005; Hellal et al., 2011). EpoB decreased scar formation in association with chondroitin sulfate proteoglycans, including NG2 proteoglycan (Cregg et al., 2014). Our study implicates that EpoB as a gene expression regulator plays a critical role in reducing scar formation after SCI.

In conclusion, EpoB is an effective reagent in decreasing scar formation and improving recovery of spinal function after SCI. The mechanisms are closely related to its function in gene regulation, especially in pericytes and fibroblasts in the injured spinal cord. More studies on the analogs of EpoB and precise gene profiling of pericytes and fibroblasts in the injured spinal cord will shed light on new treatments for SCI.

This study provides new drug intervention targets, which improve the prevention and treatment of SCI, and provides a new way of thinking SCI treatment. However, the shortcomings lie in the incomplete experiment of the relevant cells *in vitro*. Further researches are needed to prove the cell and molecular mechanisms of signal transduction pathway.

**Acknowledgments:** We appreciate Dr. Fu-zi Jin from Lunenfeld-Tanenbaum Research Institute, Mount Sinai Hospital, Toronto, Canada, for reading and revising the paper.

**Author contributions:** CY, QMF and WZ designed this study. YC, DWW and WZ performed experiments. YH, JQX and WZ analyzed data. WZ wrote the paper. All authors approved the final version of the paper.

**Conflicts of interest:** None declared.

**Plagiarism check:** This paper was screened twice using CrossCheck to verify originality before publication.

**Peer review:** This paper was double-blinded and stringently reviewed by international expert reviewers.

## References

- Alilain WJ, Horn KP, Hu H, Dick TE, Silver J (2011) Functional regeneration of respiratory pathways after spinal cord injury. *Nature* 475:196-200.
- Armulik A, Genové G, Betsholtz C (2011) Pericytes: developmental, physiological, and pathological perspectives, problems, and promises. *Dev Cell* 21:193-215.
- Ballatore C, Brunden KR, Huryn DM, Trojanowski JQ, Lee VM, Smith AB, 3<sup>rd</sup> (2012) Microtubule stabilizing agents as potential treatment for Alzheimer's disease and related neurodegenerative tauopathies. *J Med Chem* 55:8979-8996.
- Basso DM, Beattie MS, Bresnahan JC (1995) A sensitive and reliable locomotor rating scale for open field testing in rats. *J Neurotrauma* 12:1-21.
- Bergers G, Song S (2005) The role of pericytes in blood-vessel formation and maintenance. *Neuro Oncol* 7:452-464.
- Bjorklund A, Lindvall O (2000) Cell replacement therapies for central nervous system disorders. *Nat Neurosci* 3:537-544.
- Bradbury EJ, Moon LD, Popat RJ, King VR, Bennett GS, Patel PN, Fawcett JW, McMahion SB (2002) Chondroitinase ABC promotes functional recovery after spinal cord injury. *Nature* 416:636-640.
- Chen BY, You SW, Wang Y (2000) Post-operative care measures of transected rat spinal cord. *Shiyan Dongwu Kexue yu Guanli* 17:55-56.
- Cregg JM, DePaul MA, Filous AR, Lang BT, Tran A, Silver J (2014) Functional regeneration beyond the glial scar. *Exp Neurol* 253:197-207.

- Crunkhorn S (2015) CNS injury: microtubule stabilizer repairs spinal cord injury. *Nat Rev Drug Discov* 14:310.
- de Castro RJr, Tajrishi R, Claros J, Stallcup WB (2005) Differential responses of spinal axons to transection: influence of the NG2 proteoglycan. *Exp Neurol* 192: 299-309.
- Fan XH, Yang B, Hu X, Guan FX (2016) Reactive hyperplasia of glial cells induced by spinal cord injury in a rat model. *Zhongguo Zuzhi Gongcheng Yanjiu* 20:6001-6006.
- Fawcett JW (2006) Overcoming inhibition in the damaged spinal cord. *J Neurotrauma* 23:371-383.
- Fellner S, Bauer B, Miller DS, Schaffrik M, Fankhanel M, Spruss T, Bernhardt G, Graeff C, Farber L, Gschaidmeier H, Buschauer A, Fricker G (2002) Transport of paclitaxel (Taxol) across the blood-brain barrier in vitro and in vivo. *J Clin Invest* 110:1309-1318.
- Goritz C, Dias DO, Tomilin N, Barbacid M, Shupliakov O, Frisen J (2011) A pericyte origin of spinal cord scar tissue. *Science* 333:238-242.
- GrandPre T, Li S, Strittmatter SM (2002) Nogo-66 receptor antagonist peptide promotes axonal regeneration. *Nature* 417:547-551.
- Hellal F, Hurtado A, Ruschel J, Flynn KC, Laskowski CJ, Umlauf M, Kapitein LC, Strikis D, Lemmon V, Bixby J, Hoogenraad CC, Bradke F (2011) Microtubule stabilization reduces scarring and causes axon regeneration after spinal cord injury. *Science* 331:928-931.
- Kamouchi M, Ago T, Kitazono T (2011) Brain pericytes: emerging concepts and functional roles in brain homeostasis. *Cell Mol Neurobiol* 31:175-193.
- Kilkenny C, Browne WJ, Cuthill IC, Emerson M, Altman DG (2010) Improving bioscience research reporting: the ARRIVE guidelines for reporting animal research. *PLoS Biol* 8:e1000412.
- Klapka N, Hermanns S, Straten G, Masannek C, Duis S, Hamers FP, Muller D, Zuschratter W, Muller HW (2005) Suppression of fibrous scarring in spinal cord injury of rat promotes long-distance regeneration of corticospinal tract axons, rescue of primary motoneurons in somatosensory cortex and significant functional recovery. *Eur J Neurosci* 22:3047-3058.
- Kucharova K, Chang Y, Boor A, Yong VW, Stallcup WB (2011) Reduced inflammation accompanies diminished myelin damage and repair in the NG2 null mouse spinal cord. *J Neuroinflammation* 8:158.
- Lebleu VS, Taduri G, O'Connell J, Teng Y, Cooke VG, Woda C, Sugimoto H, Kalluri R (2013) Origin and function of myofibroblasts in kidney fibrosis. *Nat Med* 19:1047-1053.
- Li JF, Yan JY, Xia RF, Zhang X, Tan XH, Guan J, Ye Z, Zhang SL (2016) Glial scar formation and astrocyte role in spinal cord injury. *Zhongguo Zuzhi Gongcheng Yanjiu* 20:5609-5616.
- Liu K, Lu Y, Lee JK, Samara R, Willenberg R, Sears-Kraxberger I, Tedeschi A, Park KK, Jin D, Cai B, Xu B, Connolly L, Steward O, Zheng B, He Z (2010) PTEN deletion enhances the regenerative ability of adult corticospinal neurons. *Nat Neurosci* 13:1075-1081.
- Livak KJ, Schmittgen TD (2001) Analysis of relative gene expression data using real-time quantitative PCR and the 2<sup>-</sup>(Delta Delta C(T)) method. *Methods* 25:402-408.
- Lu P, Wang Y, Graham L, McHale K, Gao M, Wu D, Brock J, Blesch A, Rosenzweig ES, Havton LA, Zheng B, Conner JM, Marsala M, Tuszynski MH (2012) Long-distance growth and connectivity of neural stem cells after severe spinal cord injury. *Cell* 150:1264-1273.
- Okada S, Nakamura M, Katoh H, Miyao T, Shimazaki T, Ishii K, Yamane J, Yoshimura A, Iwamoto Y, Toyama Y, Okano H (2006) Conditional ablation of Stat3 or Socs3 discloses a dual role for reactive astrocytes after spinal cord injury. *Nat Med* 12:829-834.
- Pannek J, Pannek-Rademacher S, Jus MS, Krebs J (2016) Homeopathic prophylaxis for recurrent urinary tract infections following spinal cord injury: study protocol for a randomized controlled trial. *Asia Pac J Clin Trials Nerv Syst Dis* 1:191-195.
- Ren S, Johnson BG, Kida Y, Ip C, Davidson KC, Lin SL, Kobayashi A, Lang RA, Hadjantonakis AK, Moon RT, Duffield JS (2013) LRP-6 is a coreceptor for multiple fibrogenic signaling pathways in pericytes and myofibroblasts that are inhibited by DKK-1. *Proc Natl Acad Sci U S A* 110:1440-1445.
- Rolls A, Shechter R, Schwartz M (2009) The bright side of the glial scar in CNS repair. *Nat Rev Neurosci* 10:235-241.
- Ruschel J, Hellal F, Flynn KC, Dupraz S, Elliott DA, Tedeschi A, Bates M, Sliwinski C, Brook G, Dobrindt K, Peitz M, Brustle O, Norenberg MD, Blesch A, Weidner N, Bunge MB, Bixby JL, Bradke F (2015) Axonal regeneration. Systemic administration of epothilone B promotes axon regeneration after spinal cord injury. *Science* 348:347-352.
- Salgado IK, Torrado AI, Santiago JM, Miranda JD (2015) Tamoxifen and Src kinase inhibitors as neuroprotective/neuroregenerative drugs after spinal cord injury. *Neural Regen Res* 10:385-390.
- Schnell L, Schwab ME (1990) Axonal regeneration in the rat spinal cord produced by an antibody against myelin-associated neurite growth inhibitors. *Nature* 343:269-272.
- Sengottuvel V, Leibinger M, Pfreimer M, Andreadaki A, Fischer D (2011) Taxol facilitates axon regeneration in the mature CNS. *J Neurosci* 31:2688-2699.
- Silver J, Miller JH (2004) Regeneration beyond the glial scar. *Nat Rev Neurosci* 5:146-156.
- Sofroniew MV (2009) Molecular dissection of reactive astrogliosis and glial scar formation. *Trends Neurosci* 32:638-647.
- Stallcup WB (2002) The NG2 proteoglycan: past insights and future prospects. *J Neurocytol* 31:423-435.
- Tempel ZJ, Monaco EA, III, Friedlander RM (2013) Pericytes as a therapeutic target in scar formation after spinal cord injury. *Neurosurgery* 73:N18-20.
- Winkler EA, Sengillo JD, Bell RD, Wang J, Zlokovic BV (2012) Blood-spinal cord barrier pericyte reductions contribute to increased capillary permeability. *J Cereb Blood Flow Metab* 32:1841-1852.
- Xue F, Wu EJ, Zhang PX, Li-Ya A, Kou YH, Yin XF, Han N (2015) Biodegradable chitin conduit tubulation combined with bone marrow mesenchymal stem cell transplantation for treatment of spinal cord injury by reducing glial scar and cavity formation. *Neural Regen Res* 10:104-111.
- Zhang M, Chai Y, Liu T, Xu N, Yang C (2015) Synergistic effects of Buyang Huanwu decoction and embryonic neural stem cell transplantation on the recovery of neurological function in a rat model of spinal cord injury. *Exp Ther Med* 9:1141-1148.

Copyedited by Morben M, Wang J, Li CH, Qiu Y, Song LP, Zhao M